

Springer Series in Materials Science 191

Marta Castillejo
Paolo M. Ossi
Leonid Zhigilei *Editors*

Lasers in Materials Science

 Springer

Springer Series in Materials Science

Volume 191

Series editors

Robert Hull, Charlottesville, USA

Chennupati Jagadish, Canberra, Australia

Richard M. Osgood, New York, USA

Jürgen Parisi, Oldenburg, Germany

Zhiming M. Wang, Chengdu, People's Republic of China

For further volumes:

<http://www.springer.com/series/856>

The Springer Series in Materials Science covers the complete spectrum of materials physics, including fundamental principles, physical properties, materials theory and design. Recognizing the increasing importance of materials science in future device technologies, the book titles in this series reflect the state-of-the-art in understanding and controlling the structure and properties of all important classes of materials.

Marta Castillejo · Paolo M. Ossi
Leonid Zhigilei
Editors

Lasers in Materials Science

 Springer

Editors

Marta Castillejo
Instituto de Química Física Rocasolano,
CSIC
Madrid
Spain

Leonid Zhigilei
Materials Science and Engineering
University of Virginia
Charlottesville, VA
USA

Paolo M. Ossi
Departimento di Energia
Politecnico di Milano
Milan
Italy

ISSN 0933-033X

ISBN 978-3-319-02897-2

DOI 10.1007/978-3-319-02898-9

Springer Cham Heidelberg New York Dordrecht London

ISSN 2196-2812 (electronic)

ISBN 978-3-319-02898-9 (eBook)

Library of Congress Control Number: 2013955058

© Springer International Publishing Switzerland 2014

This work is subject to copyright. All rights are reserved by the Publisher, whether the whole or part of the material is concerned, specifically the rights of translation, reprinting, reuse of illustrations, recitation, broadcasting, reproduction on microfilms or in any other physical way, and transmission or information storage and retrieval, electronic adaptation, computer software, or by similar or dissimilar methodology now known or hereafter developed. Exempted from this legal reservation are brief excerpts in connection with reviews or scholarly analysis or material supplied specifically for the purpose of being entered and executed on a computer system, for exclusive use by the purchaser of the work. Duplication of this publication or parts thereof is permitted only under the provisions of the Copyright Law of the Publisher's location, in its current version, and permission for use must always be obtained from Springer. Permissions for use may be obtained through RightsLink at the Copyright Clearance Center. Violations are liable to prosecution under the respective Copyright Law. The use of general descriptive names, registered names, trademarks, service marks, etc. in this publication does not imply, even in the absence of a specific statement, that such names are exempt from the relevant protective laws and regulations and therefore free for general use.

While the advice and information in this book are believed to be true and accurate at the date of publication, neither the authors nor the editors nor the publisher can accept any legal responsibility for any errors or omissions that may be made. The publisher makes no warranty, express or implied, with respect to the material contained herein.

Printed on acid-free paper

Springer is part of Springer Science+Business Media (www.springer.com)

Preface

Lasers in Materials Science is the title of both this book and the Third International School, SLIMS-2012, held on S. Servolo Island, Venice (Italy) from July 8 to 15, 2012.

The selection of topics covered in the book and the combination of didactic introduction to the fundamentals of laser-materials interactions with up-to-date presentation of state-of-the-art techniques and emerging applications of laser processing reflect the content and spirit of the lectures and discussions at the School. One of the goals of this biennial school is to provide Ph.D. students and young research scientists working in the field of laser-materials interactions with robust fundamental knowledge that is often lacking in their training, so that they may profitably interact with colleagues working in areas neighboring their own research fields. The general area of *Lasers in Materials Science* spans fields where the interaction between laser radiation and matter plays a basic role to engineer new materials, or to enhance specific properties, mainly surface related, of irradiated matter. The laser community offers several established International Conferences where young researchers can meet with their peers, exchange experiences, establish collaborations, or display their own results to a qualified audience. However, a structured training opportunity, specifically geared toward young researchers, was lacking before the SLIMS series was established.

Focusing on the strong interplay between experimental and theoretical investigations of laser-induced phenomena, the program of the one-week residential School included 17 lectures on the fundamentals and principles of laser-materials interactions and laser materials processing. The syllabus covered the mechanisms, relevant experimental and computational techniques, as well as current and emerging applications in nanoscience, biomedicine, photovoltaics, analysis, and industry. The topics ranged from laser-surface and -bulk interactions, to the role of defects, nonlinear absorption phenomena, surface melting, vaporization, superheating, homogeneous and heterogeneous nucleation, phase explosion and plasma formation, nanosecond, femtosecond and attosecond laser pulses, film synthesis by pulsed laser deposition, nanoparticle nucleation, growth and assembling, laser nanostructuring of soft matter, development of new light and X-ray sources, free electron lasers, and laser interactions with biological tissues.

One of the distinctive features of SLIMS-2012 was the active participation of students in the activities of the School. This was facilitated by structured

classroom discussions and ample opportunity for students to discuss their ongoing projects or research plans with the School lecturers in informal settings. The students presented posters that were displayed over the School duration in the lecture hall. All posters were discussed during three extensive poster sessions and at coffee breaks. The students also gave brief oral presentations highlighting key points of their research in dedicated sessions and participated in a competition for the Best Student Presentation Award (dedicated to the memory of Prof. Roger Kelly). The School was attended by 36 students from 13 countries, with 25 students coming from EU countries, six from the USA, and four from the Mediterranean Sea area.

All lecturers, coming from both leading research centers and academic institutions, are actively involved in research topics covered by their lectures. The School Directors are grateful to School lecturers for the attention they put in the preparation of truly didactic, though high level, presentations and for the relevant work they did to convert the didactic material into self-contained book chapters that offer excellent reviews of the different topics.

Venice International University (VIU) quarters at S. Servolo Island provided superior lecturing and logistic structures in a pleasant working ambience, immersed in a quiet, beautiful garden, a few minutes from the heart of the city. This confirmed to be strategic for the success of the School.

The positive evaluation of SLIMS-2012 by the participants stimulated the planning of the forthcoming Fourth International School on *Lasers in Materials Science*, SLIMS-2014 that will be held on S. Servolo Island from July 13 to 20, 2014 under the direction of N. M. Bulgakova, Y. Lu, P. Schaaf, and P. M. Ossi.

Madrid, Spain
Milan, Italy
Charlottesville, USA

M. Castillejo
P. M. Ossi
L. V. Zhigilei

Contents

1	Laser Physics for Materials Scientists: A Primer	1
	Richard F. Haglund	
1.1	Introduction	1
1.2	Fundamentals of Laser-Materials Interactions.	4
1.3	Fundamentals of Laser Physics.	7
1.3.1	Electromagnetic Waves in a Medium with Gain and Absorption.	7
1.3.2	Creating Gain in a Laser Medium	8
1.3.3	Laser Oscillators: Theory	9
1.3.4	Mode-Locked Oscillators.	12
1.3.5	Laser Amplifiers.	13
1.4	Laser Systems Used in Materials Processing	15
1.4.1	Laser Oscillators.	15
1.4.2	Amplified Laser Systems.	20
1.4.3	Control of Laser Pulse Duration.	22
1.5	A Tunable Picosecond Laser for Polymer Processing in the Mid-Infrared	24
1.6	Conclusion.	27
	References	27
2	Material Response to Laser Energy Deposition (Thermal and Hyperthermal Processes).	29
	Juergen Reif	
2.1	Introduction	29
2.2	Basic Considerations.	30
2.2.1	Thermodynamics	31
2.2.2	Deposition of Laser Energy	32
2.3	Beyond Thermal Equilibrium (<i>Hyperthermal Processes</i>)	36
2.3.1	Homogeneous Boiling.	36
2.3.2	Ultrashort Excitation: Self-organized Nano-structure Formation	37
2.4	Summary	40
	References	41

3	Non-Thermal Material Response to Laser Energy Deposition. . . .	43
	Wolfgang Kautek and Oskar Armbruster	
3.1	Introduction	43
3.2	Response of Metals.	44
3.2.1	The Two-Temperature Model.	44
3.2.2	Hot Electron Transport	47
3.2.3	Hot Electron Pressure	49
3.2.4	Hot Electron Emission	51
3.3	Response of Dielectrics and Semiconductors	53
3.3.1	Impact/Avalanche and Multiphoton Ionization	53
3.3.2	Non-Thermal Melting	56
3.3.3	Coulomb Explosion	59
3.3.4	Photochemical Ablation.	60
3.3.5	3D Stereolithography	61
3.4	Conclusion.	62
	References	64
4	Atomic Movies of Laser-Induced Structural and Phase Transformations from Molecular Dynamics Simulations	67
	Chengping Wu, Eaman T. Karim, Alexey N. Volkov and Leonid V. Zhigilei	
4.1	Introduction	67
4.2	Representation of Laser Excitation in Classical Molecular Dynamics.	69
4.3	Atomic Movies from MD Simulations of Laser-Material Interactions	72
4.3.1	Laser Melting.	73
4.3.2	Generation of Crystal Defects	76
4.3.3	Photomechanical Spallation	81
4.3.4	Phase Explosion and Cluster Ejection	86
4.3.5	Matrix-Assisted Pulsed Laser Evaporation.	89
4.4	Concluding Remarks and Future Directions.	92
	References	94
5	Continuum Models of Ultrashort Laser-Matter Interaction in Application to Wide-Bandgap Dielectrics.	101
	Nadezhda M. Bulgakova and Vladimir P. Zhukov	
5.1	Introduction	102
5.2	Ultrafast Laser Excitation of Wide-Bandgap Dielectrics	102
5.3	Volume Modifications of Wide-Bandgap Dielectrics.	106
5.3.1	Propagation of Focused Laser Beams Through Non-linear Absorbing Media	106
5.3.2	2D Model of Electron Plasma Generation upon Laser Beam Focusing Inside Transparent Solids.	109

5.3.3	Single-Pulse Material Heating and Laser-Induced Stresses	115
5.3.4	Comments on Multipulse Irradiation Regimes	118
5.4	Concluding Remarks	120
	References	121
6	Attosecond Pulses for Atomic and Molecular Physics.	125
	Francesca Calegari, Giuseppe Sansone and Mauro Nisoli	
6.1	Introduction	125
6.2	High-Peak-Power Few-Cycle Pulses	126
6.2.1	Optical Parametric Amplification for the Generation of mJ-Energy Pulses with Stable CEP.	126
6.2.2	Hollow-Fiber Compression Technique.	127
6.2.3	High-Energy Pulse Compression by Using Gas Ionization	128
6.3	Active and Passive Stabilization of the CEP of Femtosecond Pulses	129
6.4	Generation of Isolated Attosecond Pulses	130
6.4.1	Polarization Gating	131
6.4.2	Ionization Gating	133
6.4.3	Two-Color Gating with Infrared Pulses.	134
6.5	Attosecond Metrology	135
6.6	Application of Isolated Attosecond Pulses to Molecular Physics: Electron Localization in D ₂	137
6.7	Conclusions	139
	References	139
7	Laser Interactions for the Synthesis and In Situ Diagnostics of Nanomaterials	143
	David B. Geohegan, Alex A. Puretzky, Mina Yoon, Gyula Eres, Chris Rouleau, Kai Xiao, Jeremy Jackson, Jason Readle, Murari Regmi, Norbert Thonnard, Gerd Duscher, Matt Chisholm and Karren More	
7.1	Introduction	143
7.2	Cluster and Nanoparticle Growth in Pulsed Laser Vaporization	145
7.3	Characterization and Modeling of Ultrasmall Nanoparticle “Building Blocks”.	147
7.4	Carbon Nanostructure Synthesis in Laser Vaporization	150
7.4.1	Fullerenes	150
7.4.2	Single-Wall Carbon Nanotubes	151
7.4.3	Single-Wall Carbon Nanohorns	153
7.5	Laser Diagnostics of Single-Wall Carbon Nanotube Growth by Chemical Vapor Deposition.	154

7.6	Graphene and Beyond: Laser Processing for 2D Layered Materials.	164
7.6.1	Mechanical and Chemical Exfoliation Methods and Laser Processing	164
7.6.2	Laser Interactions in the Synthesis and Characterization of Graphene and other 2D Nanosheets.	165
7.7	Summary	168
	References	169
8	Laser-Mediated Nanoparticle Synthesis and Self-Assembling	175
	Paolo M. Ossi, Nisha R. Agarwal, Enza Fazio, Fortunato Neri and Sebastiano Trusso	
8.1	Introduction	176
8.2	Propagation of an Ablation Plasma Through an Ambient Gas	177
8.3	Synthesis of Nanoparticles in the Expanding Plasma.	184
8.4	Nanoparticle Self-Assembling on a Substrate and Film Growth	189
8.5	Nanoparticle Production Via Pulsed Laser Ablation in Liquid	192
8.6	Nanoparticle Synthesis Using fs Laser Pulses.	198
8.7	Nanoparticle-Assembled Surfaces with Directed Artificial Roughness: Selected Applications.	202
8.8	Conclusions and Perspectives.	209
	References	210
9	Nano-cluster Assembled Films, Produced by Pulsed Laser Deposition, for Catalysis and the Photocatalysis.	213
	A. Miotello and N. Patel	
9.1	Introduction	214
9.2	Cobalt NPs Produced by PLD for Hydrolysis of Chemical Hydrides	214
9.2.1	Co NPs Embedded in B-Matrix Film (Co-NP-B-MA).	214
9.2.2	Co-NP-B-MA Nano-catalyst Supported Over Rough Carbon Films.	218
9.3	Co-oxide NPs Produced by PLD for Photocatalysis Application	221
9.3.1	Co ₃ O ₄ NPs Assembled Coating Photocatalyst	221
9.4	Conclusions	224
	References	224

10 Multifunctional Oxides Obtained by PLD: Applications as Ferroelectric and Piezoelectric Materials.	227
N. D. Scarisoreanu, Maria Dinescu and F. Craciun	
10.1 Introduction	228
10.2 Relaxor Ferroelectric PLZT Thin Films	232
10.2.1 PLZT 9/65/35 Thin Films	232
10.2.2 PLZT 22/20/80 Thin Films	236
10.3 Relaxor Ferroelectric PMN-PT Thin Films	243
10.4 Lead-Free SBN Thin Films	247
10.5 Lead-Free Ferroelectric NBT-BT Thin Films	258
10.6 Conclusions	263
10.7 Perspectives	264
References	266
11 Biomaterial Thin Films by Soft Pulsed Laser Technologies for Biomedical Applications	271
Ion N. Mihailescu, Adriana Bigi, Eniko Gyorgy, Carmen Ristoscu, Felix Sima and Ebru Toksoy Oner	
11.1 Introduction	272
11.2 MAPLE Set-up	273
11.3 MAPLE Layers for DDS	275
11.3.1 Bisphosphonate–Hydroxyapatite Thin Films	275
11.3.2 RNase A	277
11.3.3 Levan	282
11.4 MAPLE Layers for BS	285
11.4.1 IgG	285
11.5 MAPLE Layers for BCI	287
11.5.1 Magnesium and Strontium Doped Octacalcium Phosphate Thin Films	287
11.6 Conclusions	290
References	290
12 MAPLE and MALDI: Theory and Experiments	295
Anna Paola Caricato	
12.1 Introduction	295
12.2 MALDI: Basic Principles and Applications	297
12.3 MAPLE: Basic Principles	299
12.4 MAPLE: Applications and Influence of Deposition Parameters	304
12.4.1 Polymer Film Deposition	305
12.4.2 Maple Deposition of Bilayer Polymeric Structures	306
12.4.3 Organic Materials, Active Protein and Bioactive Thin Films	308

12.4.4	Influence of Deposition Parameters.	310
12.4.5	Deposition of Colloidal Nanoparticles/Nanorods.	314
12.5	Discussion	317
12.6	Conclusions	319
	References	320
13	Laser Nanofabrication of Soft Matter	325
	Marta Castillejo, Tiberio A. Ezquerro, Mohamed Oujja and Esther Rebollar	
13.1	Soft Matter	325
13.2	Laser Nanofabrication	327
13.3	Laser Induced Periodic Surface Structures of Thin Polymer Films	328
13.3.1	LIPSS Formation and Mechanisms	328
13.3.2	Application of LIPSS Polymer Substrates for Surface Enhanced Raman Spectroscopy	335
13.4	Laser Foaming of Biopolymer Films.	337
13.4.1	The Role of Wavelength and Pulse Duration in Laser Foaming	337
13.4.2	Cell Culture on Laser Foamed Biopolymer Films.	340
13.5	Conclusions	341
	References	342
14	Industrial Applications of Laser-Material Interactions for Coating Formation	345
	Peter Schaaf and Daniel Höche	
14.1	Introduction	345
14.1.1	The Free Electron Laser	346
14.1.2	Direct Laser Synthesis.	347
14.1.3	Protective Coatings and TiN	348
14.2	Experiments.	349
14.2.1	Sample Preparation and Setup	349
14.2.2	Analysis Methods	350
14.3	Results	350
14.3.1	FEL Irradiation at CW-Mode.	350
14.3.2	FEL Irradiation at Pulsed Mode	352
14.4	Conclusions	355
	References	356
15	Ultrafast Laser Micro- and Nano-Processing of Glasses	359
	Koji Sugioka	
15.1	Introduction	359
15.2	Surface Micromachining	361

- 15.3 Internal Modification and 3D Micro/Nanofabrication 362
 - 15.3.1 Photonic Device Fabrication 362
 - 15.3.2 Microfluidic Device Fabrication 364
 - 15.3.3 Optofluidic Device Fabrication 369
- 15.4 Processing by Pulse Shaping Technique 374
- 15.5 Summary 376
- References 377

**Erratum to: Continuum Models of Ultrashort Laser Matter
Interaction in Application to Wide-Bandgap Dielectrics E1**
Nadezhda M. Bulgakova and Vladimir P. Zhukov

Index 381

Contributors

Nadezhda M. Bulgakova Institute of Thermophysics SB RAS, Prosp. Lavrentyev, 1, Novosibirsk 630090, Russia, e-mail: nbul@itp.nsc.ru

Anna Paola Caricato Dipartimento di Matematica e Fisica “Ennio De Giorgi”, Università del Salento, Via Arnesano, 73100 Lecce, Italy, e-mail: Annapaola.Caricato@le.infn.it

Marta Castillejo Instituto de Química Física Rocasolano, CSIC, Madrid, Spain, e-mail: marta.castillejo@iqfr.csic.es

Maria Dinescu National Institute for Lasers, Plasma and Radiation Physics, Bucharest, Romania, e-mail: dinescum@ifin.nipne.ro

David B. Geohegan Center for Nanophase Materials Sciences and SHaRE Facility and Materials Sciences and Technology Divisions, Oak Ridge National Laboratory, Oak Ridge, TN 37831-6488, USA, e-mail: geohegandb@ornl.gov

Richard F. Haglund Department of Physics and Astronomy, Vanderbilt University, Nashville, TN 37235-1807, USA, e-mail: richard.haglund@Vanderbilt.Edu

Wolfgang Kautek Department of Physical Chemistry, University of Vienna, Vienna, Austria, e-mail: wolfgang.kautek@univie.ac.at

Ion N. Mihailescu Lasers Department, National Institute for Lasers, Plasma and Radiations Physics, Bucharest, Romania, e-mail: ion.mihailescu@inflpr.ro

Antonio Miotello Dipartimento di Fisica, Università di Trento, 38100 Povo, Trento, Italy, e-mail: miotello@science.unitn.it

Mauro Nisoli Dipartimento di Fisica, Politecnico di Milano, Milan, Italy, e-mail: mauro.nisoli@fisi.polimi.it

Paolo M. Ossi Dipartimento di Energia, Politecnico di Milano, 20133 Milan, Italy, e-mail: paolo.ossi@polimi.it

Juergen Reif Brandenburgische Technische Universität, BTU Cottbus, Universitaetstrasse 1, 03046 Cottbus, Germany, e-mail: reif@tu-cottbus.de

Peter Schaaf Institute of Materials Engineering and Institute of Micro- and Nanotechnologies, Ilmenau University of Technology, Gustav-Kirchhoff-Strasse 5, 98693 Ilmenau, Germany, e-mail: peter.schaaf@tu-ilmenau.de

Koji Sugioka Laser Technology Laboratory, RIKEN, Wako, Saitama 351-0198, Japan, e-mail: ksugioka@riken.jp

Leo V. Zhigilei Department of Materials Science and Engineering, University of Virginia, Charlottesville, VA, USA, e-mail: lz2n@virginia.edu

Chapter 1

Laser Physics for Materials Scientists: A Primer

Richard F. Haglund

Abstract Laser processing of materials has achieved significant successes in pulsed laser deposition, micro- and nanostructuring and surface modification and analysis. However, materials scientists often do not think about the physics of those lasers, which determines their properties and therefore also the way in which these lasers can be employed in laser processing. This chapter discusses the essential theory of laser gain, oscillation and amplification, and provides examples drawn from lasers now frequently used in materials processing. The implications for the design of new lasers and new materials-processing strategies are considered, using the example of a picosecond laser system for polymer processing.

1.1 Introduction

To optimize laser processing for specific applications and materials, it is useful to understand how lasers function, not only to select the correct lasers for particular processes, but also to provide input to laser designers and builders for new developments. In the future, an increased understanding of laser-materials interactions as these relate to laser properties will feed back into the laser-building community, to enable materials scientists to play a role in:

- Designing and constructing broadly tunable laser systems, at reasonable cost, capable of being tuned to the parameters that optimize process throughput based on fundamental laser-matter interactions;
- Understanding how the choice of amplified versus oscillator-only laser systems enables or limits the application of lasers in new processing applications as well as efficiency and overall throughput; and

R. F. Haglund (✉)
Department of Physics and Astronomy, Vanderbilt University,
Nashville, TN 37235-1807, USA
e-mail: richard.haglund@Vanderbilt.Edu

Table 1.1 Characteristics of lasers used in materials processing

Laser type	Pulse duration	Repetition frequency	Wavelength range (μm)	Fluence	Intensity
Fiber laser oscillators	CW-1 ps	CW-MHz	1.07–2.1	Modest	High
Amplified fiber lasers	Ns-fw	kHz-MHz	1.07–2.1	High	High
Diode lasers	CW- μs	CW-kHz	0.8–1.2	Modest	Low
Excimer oscillator	10–20 ns	200 Hz	0.308, 0.248, 0.193	High	Modest
Excimer amplifier	1–10 ps	10 Hz	0.248	High	High
Nd:YAG oscillators	5–20 ns	20 Hz	1.06, 0.532, 0.355, 0.266	High	Modest
Nd:YVO ₄ oscillators	5–10 ns	20 kHz	1.06, 0.532, 0.355, 0.266	Modest	Low
Yb:YAG amplifiers	0.5–20 ps	20 MHz	1.06, 0.532, 0.355, 0.266	Modest	High
Ti:sapphire oscillator	10–100 fs	100 MHz	0.7–1.0	Low	High
Ti:sapphire amplifier	100–150 fs	5 kHz	0.7–1.0	High	High
Yb:YAG + OPA	10–100 ps	1–5 kHz	0.2–20	Modest	High

- Developing figures of merit that will enable comparisons among laser systems in selecting scalable tools for applications, such as thin-film deposition, where current laser processes are not competitive with conventional processing tools.

Meeting these challenges would not only enlarge the palette of materials that can be built, assembled and fabricated using the unique electronic and vibrational interactions of light with matter, but also expand the emphasis from bulk and thin-film processing to micro- and nanoscale materials modification where the incomparable precision of laser processing holds sway.

Lasers commonly used for processing advanced materials can be categorized according to their (1) temporal pulse structure; (2) laser frequency range; and (3) tradeoffs between intensity and fluence based on pulse energy and duration. The throughput or processing rate will, as will be shown later, depends on average power. Especially during the last decade, the number of different laser types used in materials processing has expanded significantly; commercially available laser systems cover a range of all these properties, as shown in Table 1.1.

Figure 1.1 illustrates the parameter space relevant to laser processing materials, spanned by laser pulse duration and laser intensity. Solid and dashed diagonal lines show contours of constant fluence. For example, the line 1 J/cm^2 is the line representing the threshold for many laser processes initiated by pulsed nanosecond lasers, as in pulsed laser deposition. Below the line representing a fluence of 10 mJ/cm^2 , mesoscale atomic motion within a material is relatively unlikely; in this region, local phase changes and other subtle modifications to local materials properties can be achieved. Above the fluence of 100 J/cm^2 , on the other hand,

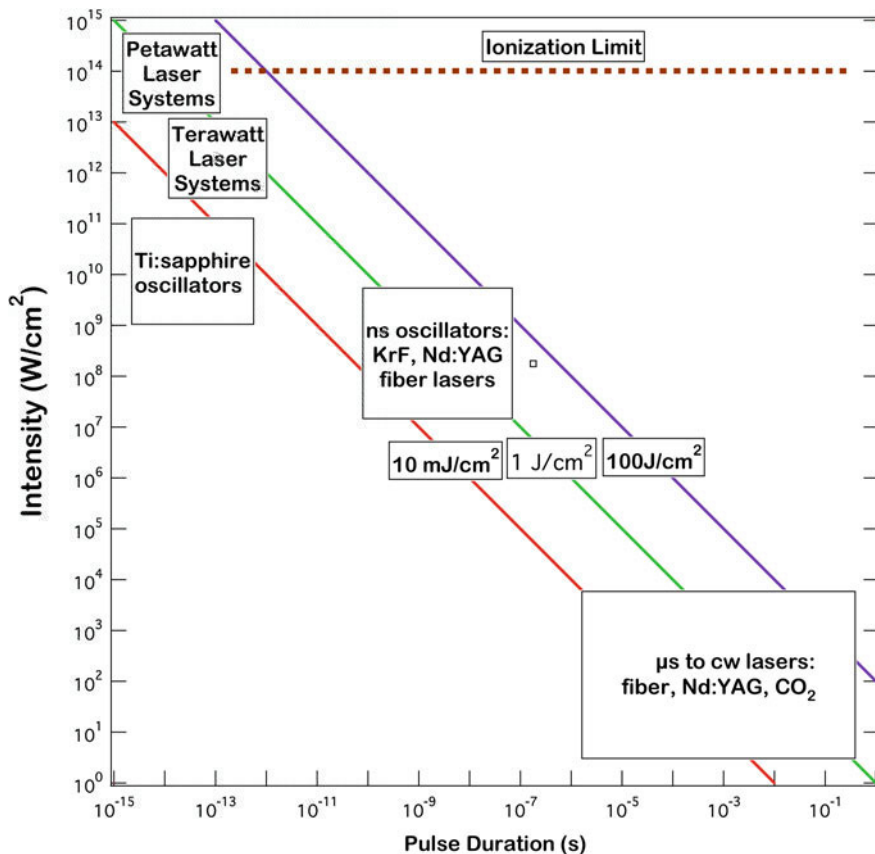


Fig. 1.1 A map of the parameter space occupied by current lasers used in materials processing. Lines of constant fluence are shown covering the range where most materials processing can occur

most materials modifications that are induced by lasers tend to be destructive for short- and ultrashort-pulse lasers, while at the limit of very long pulses, the changes tend to be thermal. As shown in Fig. 1.1, the laser systems listed in Table 1.1 nevertheless cover a wide range of the parameter space available for useful materials processing.

In this chapter, we first consider the fundamentals of laser interactions with materials as these relate to the choice of laser systems, and develop a simple figure-of-merit that makes it possible to see how various properties of a laser influence overall process throughput—and hence the economic merit of laser processing that can be compared to other processes. Next, we consider the fundamental theory of laser oscillators and amplifiers that are germane to laser processing of materials, including ways of controlling laser pulse duration and repetition frequency. Finally, we present an example of a tunable, picosecond

mid-infrared laser system based on currently available oscillators, amplifiers and parametric generators, illustrating how considering laser physics and laser properties can drive new modes of materials processing.

1.2 Fundamentals of Laser-Materials Interactions

Materials modification by lasers requires the motion of atoms, ions or molecules—which of necessity requires complex interactions in the material since photons carry very little momentum. To achieve atomic motion, three conditions must, in general, be met: First, a threshold intensity is needed to initiate the process, generally a few $\text{MW} \cdot \text{cm}^{-2}$. Second, vibrational energy—whether generated directly by infrared photon absorption or by multi-phonon cascades following electronic excitation—must be localized on a small group of atoms or a molecular-size cluster in the laser-irradiated solid for longer than a few vibrational periods. Third, the energy absorbed must be sufficient to initiate and sustain the breaking of bonds and the mesoscale motion of atoms, ions, molecules and clusters. In laser ablation, for example, the ejection of mesoscale volumes of material also creates a dense plume in which the interactions of atoms, ions, molecules and clusters with each other and with the laser light play a significant role.

Efficiency in materials modification and processing is enhanced by attending to the *hierarchical* character of laser-materials interactions. The crucial roles played by localized temporal and spatial excitation density in materials processing were first adumbrated by Stoneham and Itoh [1] and Itoh and Stoneham [2]. Their fundamental concept of localized excitation density is central to the idea of selective or non-thermal materials processing ranging from the visible-ultraviolet to the “molecular fingerprint” regions of the electromagnetic spectrum. This perspective is based on an *atomic-* or *molecular-scale* photon-matter interactions that generate *mesoscale* effects on time scales that are short compared to thermal equilibration times. Ultimately, the development of resulting in *macroscale* materials modifications on micro- to millimeter length scales.

Figure 1.2 shows schematically the sequence of processes through which the initial absorption of laser photons ultimately leads to macroscopic effects, such as those found in laser ablation, laser cutting and multiphoton structuring. By choosing the laser pulse duration or scanning speed to illuminate the target volume for a duration shorter than the thermal confinement time [3]

$$\tau_{thermal} = L_p^2 / D_{thermal} \quad (1.1)$$

(where L_{opt} is the optical penetration depth and $D_{thermal}$ is the thermal diffusivity), which in many technologically important materials is typically 0.1–10 μs , energy deposition into thermal modes of the target can be confined and the creation of a heat-affected damage zone by diffusion largely avoided, provided of course that the desired processing effect also occurs on a shorter time scale. Analogously,

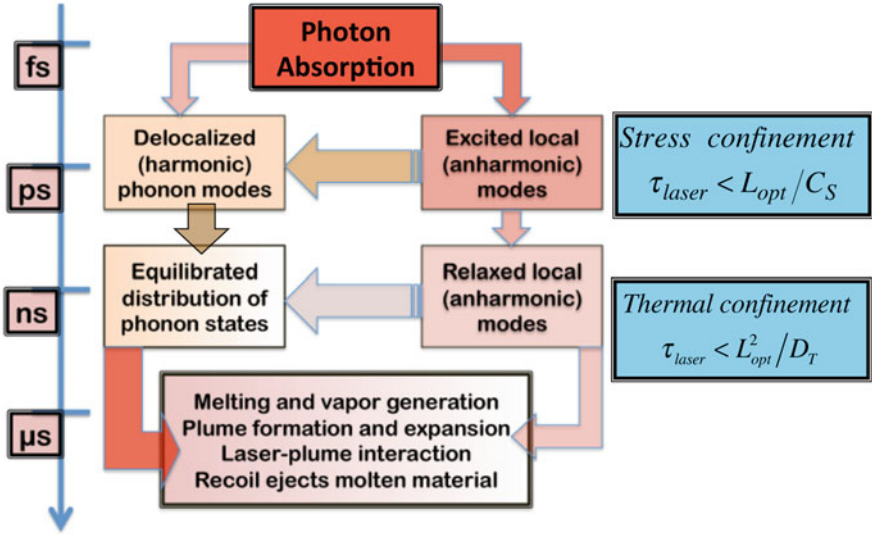


Fig. 1.2 Dynamics of photon absorption, electronic or vibrational excitation and relaxation processes leading to materials modifications such as ablation, melting and the formation of recoil-induced ejecta. The time scales relevant to stress confinement and thermal confinement are also shown

when the micropulse duration is shorter than the stress confinement time defined by [4–6]

$$\tau_{stress} = L_p / C_{sound} \quad (1.2)$$

(typically 001–0.1 μs), materials modification due to the propagation of photo-mechanically generated shock waves, spallation and exfoliation will likewise be limited to the volume in which the laser energy is absorbed.

When laser pulses excite a resonant electronic or vibrational mode of a solid, the persistence of the deposited energy in that mode and the specific relaxation mechanisms that relax or release the deposited energy determine whether or not a non-thermal process results from the laser excitation [7]. The time evolution of the laser-excited process follows from the basic quantum-mechanical result for the time rate of change of the yield of a particular process:

$$\frac{dN_0}{dt} = \eta N_0 \sigma_{(k)} \left(\frac{I}{\hbar \omega} \right)^k \quad (1.3)$$

where N_0 is the number of atoms or molecules per unit volume in the process volume, η is the quantum efficiency of the process, including loss channels; $\sigma_{(k)}$ the k th order cross section for the laser interaction with the material; and $\Phi = I / \hbar \omega$ is the photon flux, the number of photons per unit time per unit area.

From (1.3) it is evident that the rate at which a process occurs—critically important to the economics of materials processing—must then be proportional to average power. Since the probability for initiating nonlinear processes scales with powers of the intensity, rather than fluence, pulse durations of order a few picoseconds appear to have significant advantages for materials modification and processing. In particular, when the material is excited by ultrashort pulses, the initially spatially localized, anharmonic electronic or vibrational excitations are diluted only after enough time has elapsed for them to begin mixing with the delocalized, harmonic modes of the phonon bath *following* the laser pulse, whereas with nanosecond laser pulses, this relaxation begins already *during* the exciting laser pulse.

In choosing lasers for application to materials properties, it is useful to remember that the macroscopic observables—such as total yield—necessarily scale with energy deposited per unit volume (E/V):

$$Yield \propto \left(\frac{E}{V}\right) = F_L \alpha(\omega, I) \cong I_0 \tau_L [\alpha_0(\omega) + \beta \cdot I(z, t)] \quad (1.4)$$

where F_L is the laser fluence, α and β are the linear and nonlinear absorption coefficients, ω and I are the laser frequency and intensity, respectively, and z and t are the relevant space (penetration depth) and time coordinates.

The interplay of laser energy and intensity can be understood in a qualitative way by calculating the effective temperature reached in a given target volume, where the effective temperature is simply the proxy for the energy required to effect a particular materials modification. The temperature reached by absorption of a single laser pulse, the number of pulses and the rate at which they are delivered by the laser turn out to be key parameters for calculating the effect of the laser-materials interaction, assuming that the laser energy is ultimately converted into processes that eventually reach thermal equilibrium. From the analytical solution to the one-dimensional heat-conduction equation, the target temperature during a single laser pulse reaches an average value [8]

$$\langle T \rangle = \sqrt{\frac{2 I_{abs} \sqrt{a \cdot \tau_L}}{\pi \kappa}}, \quad a \equiv \frac{\kappa}{C_v \rho_0} \quad (1.5)$$

If all the absorbed energy is converted into the desired materials modification (e.g., vaporization, melting, annealing), then the specific energy input per unit volume is given by

$$\frac{E_{abs}}{V} = C_p \rho_0 \langle T \rangle = \rho_0 \Omega \quad (1.6)$$

where Ω is the binding energy per atom, another material-dependent parameter. Once thermal equilibrium is reached—typically in a few picoseconds—the temperature rise in the laser-irradiated volume as a function of laser and materials parameters can be computed as follows:

$$\Delta T = \frac{F_{abs}(\omega) \cdot \alpha(\omega, I)}{C_v \rho_0} = \frac{F_{abs}(\omega) \cdot [\alpha(\omega_0) + \beta I_{abs}]}{C_v \rho_0}, I_{abs} \tau^{1/2} = \sqrt{\frac{\pi a}{2}} \Omega \equiv f(a, \Omega) \quad (1.7)$$

The processing *rate* Y —for example, the rate of material removal in a laser ablation process leading to the deposition of a thin film—for a laser producing pulses at a rate N_{pps} with energy E_L per pulse is given by

$$Y = \eta(\omega, I) \left(\frac{E}{V} \right) N_{pps} \cong \eta(\omega, I) \frac{E_L f(a, \Omega)}{L_{opt} A(F_0, \omega)} N_{pps} \quad (1.8)$$

Here L_{opt} is the optical absorption length, $A(F_0, \omega)$ is the laser spot size at the material modification threshold for the given laser frequency, and F_0 is the threshold fluence.

From (1.8), the yield (in units of processing events per unit time) depends critically both on the materials parameters $f(a, \Omega)$ and L_{opt} , and on the pulse repetition frequency, whereas the specific energy deposition benefits from non-linear effects in the target material. Hence, it becomes virtually axiomatic that the most efficient lasers for many materials processing protocols will be high-intensity (hence ultrashort pulse), high pulse-repetition frequency devices. Optimal laser processing conditions can be achieved by choosing short optical depth, small focal spots, and high pulse-repetition frequency to achieve efficient materials modification, as reflected in (1.8) that describes the overall processing rate.

1.3 Fundamentals of Laser Physics

The characteristics of the photon beam that emerges from the laser are determined by three essential components: the gain medium, the pump or excitation source, and the optical cavity. The abbreviated treatment here illustrates how the characteristics of all three contribute to the properties of the beam, and follows the general lines found in [9]; additional details can be found in [10–12].

1.3.1 Electromagnetic Waves in a Medium with Gain and Absorption

Consider an atomic, ionic or molecular system with two energy levels, E_1 and E_2 , in thermal equilibrium. The relative population densities of the two levels N_1 and N_2 are given by Boltzmann's equation:

$$\begin{aligned}
 N_1 &= N_0 \exp[-(E_1 - E_0)/k_B T], N_2 = N_0 \exp[-(E_2 - E_0)/k_B T] \\
 \Rightarrow \frac{N_2}{N_1} &= \exp[-(E_2 - E_1)/k_B T]
 \end{aligned} \tag{1.9}$$

where k_B is the Boltzmann constant, T is the absolute temperature, and N_0 is the ground-state population density. When an electric field interacts with such a two-level atomic system, its evolution in space and time is expressed by

$$E(\omega, t) = E_0 \exp\{i[\omega t - k'(\omega)z]\} \tag{1.10}$$

The propagation constant is related to the susceptibility of the two-level medium by

$$k'(\omega) = k + k \frac{\chi'(\omega) + i\chi''(\omega)}{2n^2} - \frac{i\alpha}{2} = k + k \frac{\chi'(\omega)}{2n^2} + \frac{i\gamma(\omega)}{2} - \frac{i\alpha}{2} \tag{1.11}$$

where the vacuum wave number is k and α is the distributed loss. The optical gain or loss at the frequency ω is thus proportional to the imaginary part of the propagation constant; the sign of $\gamma(\omega)$ also depends only on the relative size of the populations in states N_1 and N_2 .

$$\gamma(\omega) \equiv k \frac{i\chi''(\omega)}{n^2} = \left[N_2 - \left(\frac{g_2}{g_1} \right) N_1 \right] \frac{\pi c^2 A_{21}}{2\omega^2} g(\omega_0, \omega) \tag{1.12}$$

As an electromagnetic wave propagates through a medium with a complex dielectric function, the change in intensity is related to the average power absorbed per unit volume by

$$\frac{dI}{dz} = - \frac{\overline{Power}}{Volume} = - \frac{\omega \epsilon_0}{2} \chi'' |E(\omega, z)|^2 = I_0 \exp\{[\gamma(\omega) - \alpha]z\} \tag{1.13}$$

Thus if the gain at any given frequency exceeds the distributed loss, the incoming wave with intensity I_0 will be amplified; if the loss dominates, an incoming electromagnetic wave will be attenuated. The key to making a successful laser oscillator or amplifier is therefore to create a population inversion that makes the factor in braces in (1.13) positive; the second is to reduce the distributed losses α due to scattering, reflection and absorption in the laser medium and the optical resonator to a minimum.

1.3.2 Creating Gain in a Laser Medium

In any system of atoms, ions or molecules in thermal equilibrium, the population in state 2 is always exponentially less than that in state 1. Hence, creating gain, rather than loss, in a laser medium requires the creation of a highly non-equilibrium distribution of atoms. This is the function of the laser “pump,” which may be

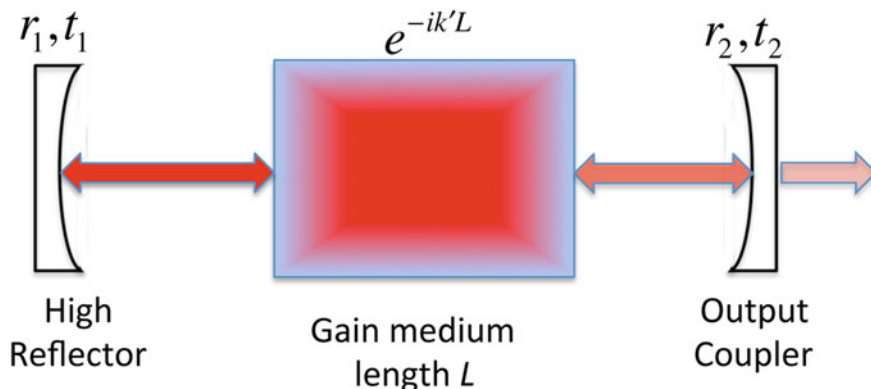


Fig. 1.3 Schematic of a Fabry–Perot resonator, showing how phase and amplitude accumulate with increasing numbers of round trips through the cavity

a flashlamp, an electron beam, an electric discharge, an electric current or even another laser. While flashlamps and electric discharges are still used in many nanosecond laser oscillators, the development of high-efficiency laser diodes operating in the near infrared has made optical pumping an increasingly popular choice, especially for mode-locked and fiber lasers, because of the uniformity and stability of their output and the efficiency with which the diode lasers can be coupled directly into the desired pump transition.

1.3.3 Laser Oscillators: Theory

The possibility of light amplification by stimulated emission leads naturally to the question of how to build an oscillator—that is, an optical device in which a very small input signal can grow into a self-sustaining optical beam, either continuous or pulsed. Such an oscillator may be either pulsed or continuous-wave (CW); regardless of which it is, the basic principles remain the same. As a model system (Fig. 1.3), we consider a simple laser cavity with a gain medium of length L , which is essentially a pair of resonator mirrors that are perfectly aligned. For the sake of definiteness, we assume that one mirror is a high reflector, with reflection and transmission coefficients (r_1, t_1) , while the other mirror, the output coupler, is partially transmitting with coefficients (r_2, t_2) . If we imagine the initially infinitesimally small light signal E_0 entering through mirror 1, with transmission coefficient t_1 , by the time it passes through mirror 2 with transmission coefficient t_2 it has acquired an additional phase $\exp(-ik'L)$ that has both real and complex components and also incorporates the effects of optical gain at frequency ω and the distributed loss α . Describing the electric field in complex exponential notation, we can write the output wave as an infinite series of waves reflected back and forth

within the Fabry–Perot cavity while allowing for partial transmission of the wave at mirror 2, as shown in Fig. 1.3. Summing the series yields

$$E_t = E_0 t_2 t_1 e^{-ik'L} \left(1 + r_2 r_1 e^{-2ik'L} + r_2^2 r_1^2 e^{-4ik'L} + \dots \right) = \frac{E_0 t_2 t_1 e^{-i(\bar{k} + \Delta k)L} e^{(\gamma - \alpha)L/2}}{1 - r_2 r_1 e^{-2i(\bar{k} + \Delta k)L} e^{(\gamma - \alpha)L}} \quad (1.14)$$

For laser oscillation to occur, it is necessary that the denominator of this equation approach zero, so that a finite output can be generated by amplification of an infinitesimally small input signal. This can happen when the denominator vanishes, leading to two conditions for oscillation, one on the threshold gain required to overcome the distributed losses in the cavity, and the other on the phase of the waves:

$$\begin{aligned} r_1 r_2 \exp \{ [\gamma_{th}(\omega) - \alpha]L \} &= 1 \text{ (amplitude) and} \\ 2[k + \Delta k(\omega)]L &= 2\pi m, \quad m \text{ an integer (phase)} \end{aligned} \quad (1.15)$$

The phase condition effectively guarantees that a standing electromagnetic wave will be generated in the resonant cavity, and the amplitude condition says that the wave will grow in amplitude as long as the gain exceeds the threshold value. The m th frequency at which the cavity will oscillate can be derived from the phase condition to be:

$$[k + \Delta k(\omega)]L = kL \left[1 + \frac{\chi'(\omega)}{2n^2} \right] = m\pi \Rightarrow \omega_m = \omega \left[1 - \frac{\omega - \omega_0}{\Delta\omega} \frac{\gamma(\omega)}{k} \right] \quad (1.16)$$

If the laser resonator has a photon lifetime τ_0 , we can use this to calculate the threshold population inversion as well, assuming that the population in the level N_1 is initially negligible:

$$\tau_0 = \frac{2nL}{c(1 - R_1 R_2 e^{-2\alpha L})} \approx \frac{2nL}{c[2\alpha L - \ln(R_1 R_2)]} \Rightarrow N_{2threshold} = \frac{8\pi}{A_{21} \lambda^2 g(v) c \tau_0} \quad (1.17)$$

In laser oscillators typical of those used in most materials-processing applications, the mechanism described here results in the emission of a laser pulse that will persist until the population inversion has been extinguished, typically on a time comparable to the photon lifetime in the cavity (1.17). Figure 1.4 shows how the longitudinal modes of a Fabry–Perot cavity are modulated by the gain profile of the laser medium. Those modes on which the *net* gain exceeds the lasing threshold as defined by (1.15) will oscillate randomly; in a kind of Darwinian competition, various modes will oscillate until all are driven down to the threshold gain level.

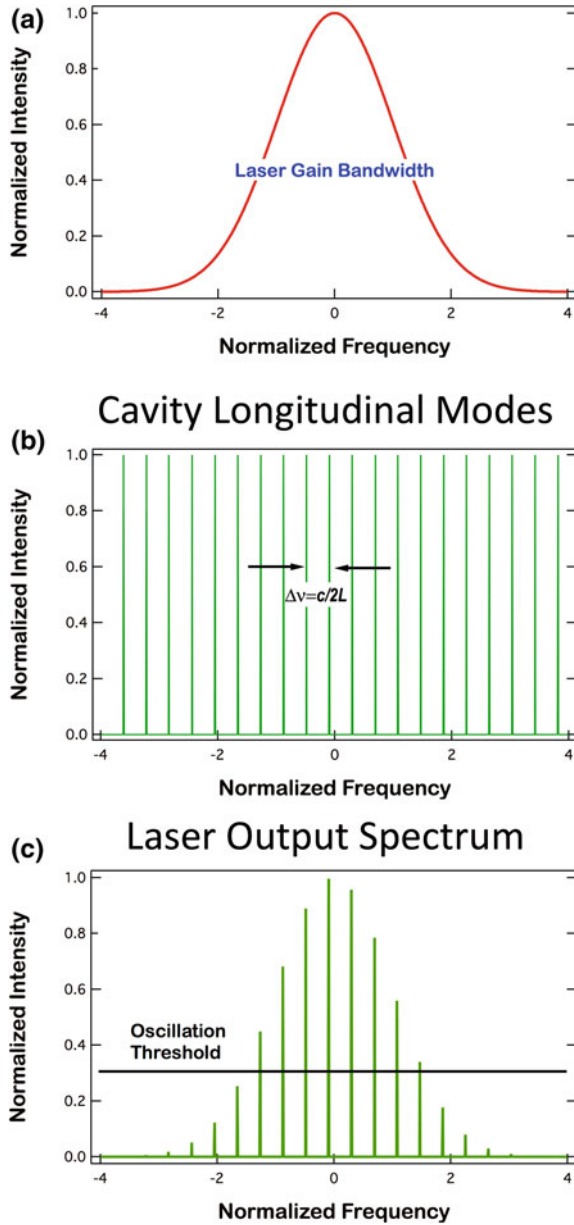


Fig. 1.4 **a** Schematic laser gain profile, derived from the atomic or molecular laser line. **b** Longitudinal cavity modes, spaced by the inverse of the cavity round-trip time. **c** Output spectrum convoluting the cavity modes with the laser gain profile; those modes that have intensity above threshold all cavity modes can lase in competition with one another

1.3.4 Mode-Locked Oscillators

Because the gain created in the excitation cycle is subject to statistical fluctuations, there may be substantial pulse-to-pulse variations in duration and energy. However, there is another approach that is designed to minimize these fluctuations, called *mode-locking*. The fundamental idea of mode-locking is the following: At a given frequency ν , the gain $\gamma(\nu)$ satisfies

$$\gamma_{\text{threshold}}(\nu) = \alpha - \frac{1}{L} r_1 r_2 \Leftrightarrow \gamma(\nu) = (N_2 - N_1) \frac{c^2}{8\pi n^2 \nu^2 \tau_{\text{spont}}} g(\nu) \quad (1.18)$$

Moreover, we know that wherever the gain at a given frequency is sufficient to overcome the losses in the optical cavity, laser oscillations can occur over a range of frequencies ν_q defined by

$$\nu_{q+1} - \nu_q = \frac{c}{2nL} \text{ or } \omega_q - \omega_{q-1} = \frac{\omega c}{L} \equiv \Omega \quad (1.19)$$

In essence, as long as there is sufficient gain, all the frequencies that differ from each other by the inverse of the round-trip propagation time in the cavity can oscillate. The total electric field at some arbitrary point in the cavity can be made periodic in the cavity round-trip time

$$E(t) = \sum_n E_n \exp[i(\omega_0 + n\Omega)t + \phi_n] = E(t + T), T = \frac{2\pi}{\Omega} = \frac{2L}{c} \quad (1.20)$$

provided that the phase ϕ_n , which normally fluctuate in a random fashion in the cavity, can be made equal to each other, that is *locked*. In this circumstance, the cavity modes E_n all have the same phase relationship with each other, and if the amplitude of all the electric field modes is constant, the total electric field is

$$E(t) = \sum_{-(N-1)/2}^{+(N-1)/2} E_0 \exp[i(\omega_0 + n\Omega)t] = \exp[i\omega_0 t] \frac{\sin(N\omega t/2)}{\sin(\omega t/2)} \quad (1.21)$$

where ω_0 is the frequency at the center of the gain profile. The average oscillator output power, which is proportional to the square of the electric field, is then given by

$$P(t) \propto |E(t)|^2 = \frac{\sin^2(N\omega t/2)}{\sin^2(\omega t/2)} \quad (1.22)$$

What this means is that the power is emitted in a train of pulses separated from other by the cavity round-trip time, and where the individual pulse duration is $2L/cN$. Just as the intensity of light from N coherently interfering apertures is N^2 times the intensity from a single aperture, the power from N interfering modes is N^2 times the power from a single mode. Moreover, the pulse duration, approximated as the time from the peak to the first zero of the mode-locked train, is $1/N$ times the

round-trip time T . Estimating the number of oscillating modes as the ratio of the transition linewidth $\Delta\omega$ to the intermode frequency spacing Ω , the pulse duration τ_0 is

$$\tau_0 \sim \frac{2\pi}{\Delta\omega} = \frac{1}{\Delta\nu} \quad (1.23)$$

Hence the larger the transition linewidth for the laser transition is, the shorter is the pulse that can be obtained by mode-locking. Importantly, in solid-state laser materials, this linewidth depends not only on the lasing atom or ion, but also on the host material in which the optically active ion is embedded. In addition, since the laser is being pumped continuously, the pulse-to-pulse variation in the mode-locked train tends to be substantially smaller than in laser oscillators in which the pumping or excitation cycle produces a single output pulse.

As long as the mode-locked laser cavity is continuously excited, pulses will be generated continuously at a frequency $c/2L$, which for typical cavity dimensions of tens of centimeters leads to pulse repetition frequencies from tens of MHz to a few GHz. The energies of these pulses are usually in the nJ range and must therefore be amplified to reach the typical J/cm^2 fluences required for laser processing. However, at the very highest pulse-repetition frequencies, even the thermal loading produced by the oscillator pulses is often unacceptably high, creating a requirement either to scan the beam at high speeds so that the requirements of thermal and stress confinement are satisfied, or to reduce the pulse-repetition frequency to an acceptable level. This is generally accomplished by time-dependent modification of the resonant cavity, as will be explained below.

1.3.5 Laser Amplifiers

The majority of lasers used in materials processing are oscillators, either continuous-wave (such as diode lasers) or pulsed. However, increasingly the advantages of mode-locked oscillators—pulse durations in the femtosecond and picosecond range, and excellent power stability—are generating interest in their use in materials processing. The chief difficulty with that is the output of mode-locked oscillators comes at very high pulse-repetition frequencies, leading to undesirable thermal loading for some applications, but very low pulse energies. This leads to the need for amplification.

We assume for purposes of discussion that we are dealing with a two-level system, and that for simplicity, the amplifier medium is homogeneously broadened. Then the processes we need to deal with are: the pumping rates per unit volume into level 2 and level 1, the radiative decay from those two levels, stimulated absorption or emission on the laser transition arising from interaction with a beam of radiation, and the population of the lower level by the process of spontaneous emission. With these assumptions, it is possible to write down a pair of rate equations that describe the time evolution of these two levels.

$$\begin{aligned}\frac{dN_2}{dt} &= R_2 - N^* \sigma_{21} (\omega_L - \omega_0) \frac{1}{\hbar \omega_L} - \frac{N_2}{\tau_2}, \quad \text{where } N^* \equiv N_2 - \frac{g_2}{g_1} N_1 \\ \frac{dN_1}{dt} &= R_1 - N^* \sigma_{21} (\omega_L - \omega_0) \frac{1}{\hbar \omega_L} - \frac{N_1}{\tau_1} + N_2 A_{21}\end{aligned}\quad (1.24)$$

Assuming that we are in a steady state, that is, that the lifetimes are long compared to whatever processes lead to loss of inversion, we have

$$\left. \begin{aligned} N_2 &= R_2 \tau_2 - N^* \sigma_{21} \frac{I}{\hbar \omega_L} \tau_2 \\ N_1 &= R_1 \tau_1 + N^* \sigma_{21} \frac{I}{\hbar \omega_L} \tau_2 + N_2 A_{21} \tau_1 \end{aligned} \right\} \Rightarrow N^* = \frac{R_2 \tau_2 [1 - (g_2/g_1) A_{21} \tau_1] - (g_2/g_1) R_1 \tau_1}{1 + \sigma_{21} \frac{I}{\hbar \omega_L} [\tau_2 + (g_2/g_1) \tau_1 (1 - A_{21} \tau_2)]}\quad (1.25)$$

Since this inversion density basically determines the magnitude of the gain and its duration, we can now notice that the numerator in the equation for N^* is the gain in the absence of the radiation field, which we denote $N^*(0)$, while the denominator contains a time-dependent term which is essentially the relaxation time for the population inversion:

$$\begin{aligned} N^*(I) &= \frac{N^*(0)}{1 + \frac{I}{I_{sat}(\omega_L - \omega_0)}} \\ I_{sat}(\omega_L - \omega_0) &\equiv \frac{\hbar \omega_L}{\tau_R} \frac{1}{\sigma_{21} (\omega_L - \omega_0)}, \quad \tau_R \equiv \tau_2 + \frac{g_2}{g_1} \tau_1 [1 - A_{21} \tau_2]\end{aligned}\quad (1.26)$$

The saturation intensity I_{sat} is a measure of how much the population inversion is affected by the presence of radiation in the cavity: If $I \ll I_{sat}$, the population inversion is changed very little by the intensity in the cavity; if $I \gg I_{sat}$, then the population inversion is strongly depleted by the presence of the radiation in the cavity. These (1.25) can be recast into a particularly useful form if we define a net pumping rate R^* , leading to an expression for the inversion rate per unit volume

$$\frac{dN^*}{dt} = R^* - \left(1 + \frac{g_2}{g_1}\right) \frac{N^* I}{\tau_R I_{sat}} + \text{spontaneous emission terms}\quad (1.27)$$

In any of the lasers commonly used in materials processing, the spontaneous emission terms are small compared to the other two terms, and can be safely neglected. Equation (1.26) essentially states that the inversion rate—which determines the gain—is proportional to the pumping rate diminished by a term that is inversely proportional to the relaxation time and directly proportional to the laser intensity in the cavity.

The practical effect of this situation for a laser amplifier is that as the intensity in the amplifier increases, the intensity gain for light traversing the amplifier in the z direction changes from exponential in the small-signal region to linear in the saturated region: